Osteoarthritis and Cartilage 21 (2013) 551–558

Osteoarthritis and Cartilage

Increased acetabular subchondral bone density is associated with cam-type femoroacetabular impingement

A.D. Speirs †, P.E. Beaulé ‡, K.S. Rakhra §, M.E. Schweitzer §, H. Frei †*

† Department of Mechanical and Aerospace Engineering, Carleton University, Ottawa, ON, Canada
‡ Division of Orthopaedic Surgery, The Ottawa Hospital, Ottawa, ON, Canada
§ Department of Medical Imaging, The Ottawa Hospital, Ottawa, ON, Canada

ARTICLE INFO

Article history:
Received 20 August 2012
Accepted 18 January 2013

Keywords:
Osteoarthritis
Subchondral bone
Femoroacetabular impingement
Hip
Quantitative CT

SUMMARY

Objective: Femoroacetabular impingement (FAI) has been associated with significant acetabular cartilage damage and subsequent degenerative arthritis. Subchondral bone, often neglected in osteoarthritis studies, may play an important role in the degenerative cascade. Hence the goal of this study was to assess acetabular subchondral bone mineral density (BMD) in subjects with asymptomatic or symptomatic cam deformities compared to normal control subjects. The relationship between BMD and the alpha angle, a quantitative measure of the deformity, was also analyzed.

Methods: Patients diagnosed with symptomatic cam FAI were recruited ('Surgical') as well as subjects from the general asymptomatic population, classified from CT imaging as normal ('Control') or having a cam deformity ('Bump') based on their alpha angle measurement. There were 12 subjects in each group. All subjects underwent a CT scan with a calibration phantom. BMD was calculated in regions of interest around the acetabulum from CT image intensity and the phantom calibration. BMD was compared between groups using spine BMD as a covariate. The relationship between BMD and alpha angle was assessed by linear regression.

Results: In the antero-superior regions bone density was 15–34% higher in the Bump group ($P < 0.05$) and 14–38% higher in the Surgical group ($P < 0.05$) compared to Controls. BMD correlated positively with the alpha angle measurements ($R^2 = 0.44$, $P < 0.001$).

Conclusion: BMD was elevated in subjects with cam-type deformities, with the severity of the deformity more correlative than symptom status. Similarities to the symptomatic group suggest that hips with an asymptomatic deformity may already be in early stages of joint degeneration.

Introduction

Although osteoarthritis is a well recognized degenerative condition of articular joints, the underlying pathomechanism is not well understood. Brandt *et al.* noted that consensus definitions typically describe late-stage joint condition and focus on alterations in the hyaline cartilage thickness, composition and properties[1]. However osteoarthritic degeneration is a complex process and can involve any or all tissues of the joint such as the synovium and subchondral bone in addition to the cartilage[2,3].

Although much work has focused on degeneration and treatment of cartilage, some studies have suggested the subchondral bone may play an important and early role in the osteoarthritic cascade[1,3]. In later stages of the disease, increased bone density is recognized clinically as sclerosis on plane radiographs which has a strong association with osteoarthritis[4–6]. Sclerosis is in fact an important criterion in the well-established Kellgren–Lawrence and Tönnis grading systems of osteoarthritic joints[4,5]. Sclerosis is typically evaluated as either present or absent[6,7] and planar analyses of the hip such as with X-ray or Dual-energy X-ray absorptiometry (DEXA) do not provide quantitative, spatially-varying information on bone changes due to overlapping structures on the projection view. Quantitative analyses may reveal subtle changes specifically at the level of the subchondral bone in early stages of degeneration[8]. Furthermore subchondral bone changes and markers of remodelling were found to precede biochemical changes in cartilage[3,9]. These changes may therefore be an early marker of osteoarthritic degeneration.

* Address correspondence and reprint requests to: H. Frei, Department of Mechanical and Aerospace Engineering, Carleton University, 1125 Colonel By Dr, Ottawa, ON, Canada K1S 5B6. Tel: 1-613-520-5686; Fax: 1-613-520-5715.
E-mail addresses: andrew_speirs@carleton.ca (A.D. Speirs), pbeaule@ottawahospital.on.ca (P.E. Beaulé), krakhra@ottawahospital.on.ca (K.S. Rakhra), mschweitzer@toh.on.ca (M.E. Schweitzer), hfrei@mae.carleton.ca (H. Frei).

1063-4584/$ – see front matter
http://dx.doi.org/10.1016/j.joca.2013.01.012

Femoroacetabular impingement (FAI) has recently been identified as a clinically-relevant condition, and may be responsible for up to 90% of adult idiopathic hip osteoarthritis[10]. In cam-type FAI, a convex deformity of the antero-superior femoral head–neck junction can result in repeated abnormal contact between the femur and the antero-superior acetabular rim and labrum, leading to degeneration and eventual cleavage of the cartilage layer[10]. The cam deformity is quantified by measurement of the alpha angle, which was originally described by Nötzli *et al.* on axial oblique MR images[11] (Fig. 1). Incidental cam deformities have been reported in 14% of volunteers recruited from the general asymptomatic population[12] as well as in patients with surgically proven unilateral cam FAI where up to 59% can have a cam deformity in the asymptomatic contralateral hip[13]. The hip joint with an asymptomatic cam deformity may already be in an early stage of degeneration and analysis of these pre-clinical FAI joints could provide important *in vivo* information about the early degenerative processes.

The overall hypothesis is that impingement between the cam deformity and the acetabular rim and labrum is leading to an elevated subchondral bone density in the acetabulum. The primary goal of this study was thus to examine subchondral bone density in the acetabulum in subjects with symptomatic cam-type FAI or asymptomatic cam deformity, as compared to normal controls. Further, the relationship between bone density and the alpha angle was analyzed using linear regression. It is hypothesized that subjects with a cam deformity will exhibit higher subchondral bone density than controls, and that this elevated density is correlated with a higher alpha angle.

Materials and methods

Subjects

Twelve symptomatic cam-type FAI subjects were recruited from the clinical practice of one of the authors ('Surgical' group) and prior to surgery underwent computed tomography (CT) imaging of the hip. Age-matched asymptomatic volunteers were recruited from the general population and categorized as asymptomatic cam deformity ('Bump' group) or asymptomatic normal ('Control' group) based on the alpha angle as described below (Table I). The study was conducted in accordance with the Helsinki declaration and approved by the research ethics board of the hospital. All subjects provided written informed consent prior to being enrolled.

Table I
Patient demographics. Alpha angle shown is from the 3:00 plane

Group	*n* (M:F)	Alpha angle (Mean ± SD)	Age (mean, range)	Weight (kg, mean ± SD)
Control	12 (8:4)	44.9° ± 3.6°	33.3 (25.0–42.0)	82.0 ± 15.8
Asymptomatic	12 (11:1)	55.6° ± 9.2°	31.9 (25.7–44.3)	81.0 ± 13.9
Surgical	12 (12:0)	57.3° ± 8.4°	37.7 (25.3–50.9)	88.4 ± 19.5

Patient measurements

All subjects underwent bilateral quantitative CT (qCT) scans with a calibration phantom (Model 3, Mindways Software, Austin, TX, USA) covering from the iliac crest to the lesser trochanter. Slices were acquired with settings of 120 kVp, 200 mAs, a thickness of 0.5–0.625 mm and a 512 × 512 matrix resulting in an in-plane resolution of 0.72–0.98 mm, depending on the size of the subject. Two CT scanners were employed during the test, a Toshiba Aquilion and GE Discovery CT750. Bone cement and an epoxy-resin femur were scanned with the phantom in each scanner and the CT-equivalent density of the objects differed by less than 5 mg/cc. All CT scans were reconstructed using a bone window of the respective manufacturer. CT images were acquired in the axial plane and used to generate oblique coronal planes parallel to the femoral neck axis. The oblique coronal image was then used to prescribe an oblique axial image parallel to the femoral neck axis (Fig. 1), called the 3:00 plane[11,14] and is used for measurement of the traditional alpha angle[11]. An oblique sagittal image, perpendicular to the femoral neck axis through the subcapital zone of the femoral neck was used to prescribe the radial series of images using the femoral neck axis as the axis of rotation, described by Rakhra *et al.*[14] An image in the 1:30 plane was generated corresponding to a 45° rotation of the 3:00 plane (Fig. 1) as described by Rakhra *et al.*[14] The alpha angle was then measured on two images to evaluate the femoral head–neck junction anteriorly and antero-superiorly in the traditional axial oblique[11] (3:00) and 1:30 planes, respectively. Asymptomatic subjects with an alpha angle greater than or equal to 50.5° measured in the 3:00 plane[15,16] or greater than 60° in the 1:30 plane were classified as 'Bump' whereas subjects with both alpha angles less than the respective thresholds were classified as 'Control'. The threshold in the 3:00 plane was found to be 100% accurate identifying the presence of a cam deformity in a series of symptomatic hips when compared

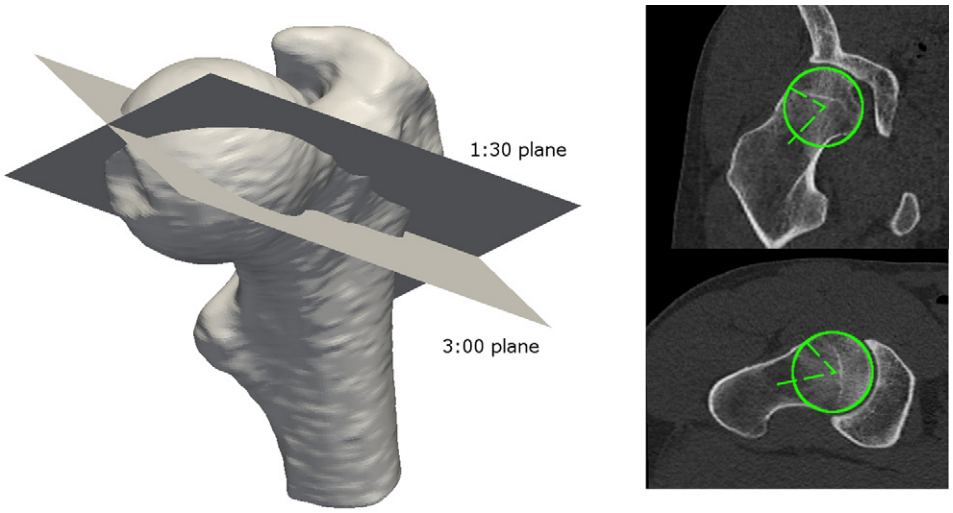

Fig. 1. Left: The 1:30 and 3:00 planes used for measurement of the alpha angle. The planes intersect along the neck axis. Right: Reformatted CT slices showing the alpha angle measurements in the 1:30 (top) and 3:00 (bottom) planes.

with intraoperative findings[16], whereas the 60° threshold in the 1:30 plane was recently proposed as a compromise between sensitivity and specificity in distinguishing symptomatic cam deformities[17].

Bone density measurements

To examine the spatial variation in density differences, bone mineral density (BMD) was determined in regions around the acetabulum and at varying depths from the rim as follows. The acetabular region of both hips of each subject was semi-automatically segmented (ITK-Snap, v2.2, itksnap.org). To standardize regions for bone density analysis, the acetabular rim plane (ARP), anterior pelvic plane (APP) and hip centre were defined (Fig. 2)[18]. ARP, a virtual plane, was defined by selecting the most antero-lateral and postero-lateral points on the acetabular rim identified on axial CT slices through the superior–inferior depth of the acetabulum as described by Lubovsky *et al.*[18] ARP was then calculated as a least-squares best-fit plane of these points, which included at least 30 points for each patient. APP was determined by the left and right anterior superior iliac spines and the mid-point of the pubic tubercles. The hip centre and radius were determined from a least-squares best-fit sphere of the subchondral horseshoe-shaped bearing surface area of the segmented surface model. The local transverse plane was defined perpendicular to the ARP and APP and contained the hip centre (Fig. 3). The acetabular surface model was trimmed to a depth of 10 mm by intersection with a sphere centred on the hip centre, a thickness approximately an order of magnitude larger than a typical voxel diagonal (Fig. 3). The intersected region was then divided into 12 equal wedge-shaped sections by rotating the local transverse plane around the ARP normal in 30° increments using custom software (Fig. 3). Regions varied from approximately 0.6–1.6 cm^3. Subsequently a mesh was created in each of the resulting acetabular wedges (Netgen Mesh Generator, v4.9.13, http://sourceforge.net/apps/mediawiki/netgen-mesher) consisting of approximately 100,000 tetrahedra per wedge. Two planes parallel to the ARP were used to divide the 12 acetabular wedges into three depth levels, i.e., the rim, middle and medial wall (Fig. 3). The wedges were divided at a distance from the hip centre of one-third and two-thirds of the best-fit acetabular radius. Each tetrahedral element in a wedge was then assigned to the corresponding depth level based on the location of the element centroid.

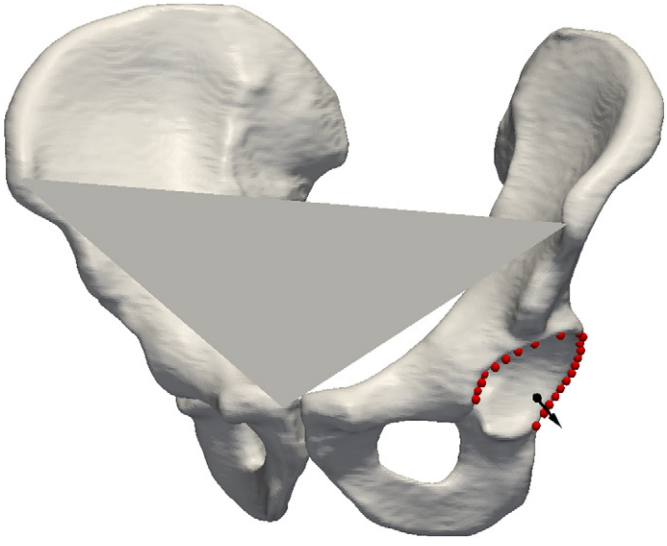

Fig. 2. Geometry definitions used to standardize the regions of interest in the acetabulum. The APP (triangle) was defined by the left and right anterior superior iliac spines and the mean of the coordinates of the pubic tubercles. The ARP was calculated from a best-fit plane of points on the rim (red). The black arrow represents the normal to the ARP. The sphere at the base of the arrow marks the centre of the acetabular best-fit sphere.

Each CT scan was calibrated according to the phantom manufacturer's directions. For each subject the linear relationship between CT image intensity (Hounsfield Units or HU), and K_2HPO_4-equivalent bone density was calculated by measuring the average HU in five tubes in the phantom and performing a linear regression with K_2HPO_4 values provided by the manufacturer's calibration certificate. HU was sampled in each element using the SampleScalarField function in Amira (Amira v5.4, Visage Imaging Inc, San Diego, USA) and converted to bone density using the relationship established by the calibration. The average bone density in each level of each wedge was calculated as the volume-average density of the corresponding elements. The bone density was therefore analyzed in 36 regions of interest i.e., three levels in each of 12 wedges. The effect of element size on mean density values per wedge was examined by generating a mesh in 12 wedges of seven subjects with approximately 15,000 elements per wedge. Absolute differences between mean values ranged from 0.15 to 1.0 mg/cc across all wedges. Reproducibility of the measurements was assessed by randomly selecting the affected hip of two subjects in each group and repeating the entire process by the same observer. Test–retest differences per zone were typically less than 10 mg/cc. The mean absolute difference was 7 mg/cc.

Since study subjects were expected to exhibit general bone density differences e.g., due to body weight, activity level, genetics, diet etc, a small spherical region was segmented, approximately 1.6 cm^3, in the cancellous bone of the fifth lumbar vertebral body. The average HU in this region was converted to bone density from the calibration and used as a covariate in statistical analyses. The location was chosen such that it could be included in the scan without substantially increasing the radiation dose but was sufficiently remote from the hip joint so as not to be affected by impingement. This bone density variable is referred to as L5.

Statistical analysis

Differences in bone density between Control, Bump and Surgical groups were examined in each of the 36 regions using a one-way analysis of covariance (ANCOVA), with study group as the single factor and L5 density the covariate. L5 was confirmed to be a significant covariate in all regions. With the exception of three regions in the inferior acetabulum, the L5 density × group interaction term was not significant, indicating a single regression slope could be applied for all covariate corrections. The exceptions were confined to the inferior fossa and were composed primarily of the thin medial border of the acetabulum and pelvis. This was considered to be of minimal interest in hip biomechanics, thus no attempt was made to account for heterogeneous regression slopes in the ANCOVA test for those three regions. If group was a significant factor in the overall ANCOVA result in a region ($P < 0.05$), differences between specific groups were analyzed using a Student's t test with a Sidak correction for three comparisons in order to maintain an overall Type I error rate of 0.05 within each zone. To determine whether bone density differences between groups were related to the alpha angle, a step-wise linear regression was performed between bone density vs alpha angle and L5 in the antero-superior and adjacent regions (sections 12 and 1–4) where cartilage damage or delamination is typically seen intraoperatively. An independent variable was removed in the step-wise analysis if the probability of the associated change in F-statistic exceeded 0.1. A simple linear regression was also performed to show the effect of alpha angle alone. Since cam deformities often occur bilaterally[12,13]

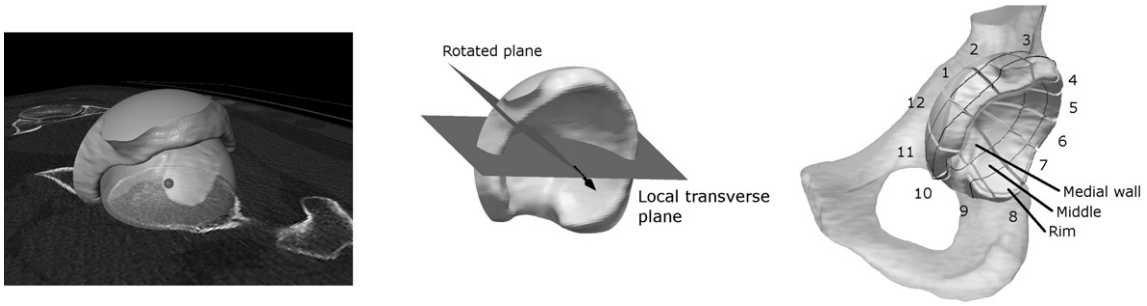

Fig. 3. Left: Segmented acetabular region of a left hip with axial CT slice shown semi-transparent. Also visible is the best-fit sphere and the sphere centre (small black sphere). Middle: The acetabular region was created from the pelvis by intersection with a sphere. This was divided into wedge sections by rotating the local transverse plane about the normal of the ARP (black arrow). Right: The acetabulum was divided into 12 wedge-shaped sections shown exploded, where section 1 is anterior. Each section was subdivided into rim, middle and medial wall levels based on the perpendicular distance from the ARP.

a subgroup analysis was performed to examine within-subject differences in BMD associated with the cam deformity. From the Bump group, all subjects with a unilateral deformity were included as one subgroup i.e., subjects in which the contralateral 3:00 and 1:30 angles were below 50.5° and 60°, respectively ($n = 6$). In the Surgical group all subjects exhibited bilateral deformities and were included in the within-subject analysis ($n = 12$). Due to the small sample size in the Bump group a Wilcoxin matched-pairs signed-ranks test was performed to detect differences between the affected and contralateral normal sides. A paired-samples *t*-test was performed in Surgical subjects in each region to compare differences between the affected and contralateral side. Since these tests involved within-patient factors, no adjustment for a covariate was necessary. All analyses were performed using SPSS Statistics, v17 (IBM Corp, NY, USA).

Results

Bone density: rim level

Bone density was generally higher in both Bump and Surgical groups compared to Controls, especially in the antero-superior quadrant (sections 1–3) of the acetabulum [Fig. 4(a) and Table II] as well as some adjacent regions. In the antero-superior quadrant,

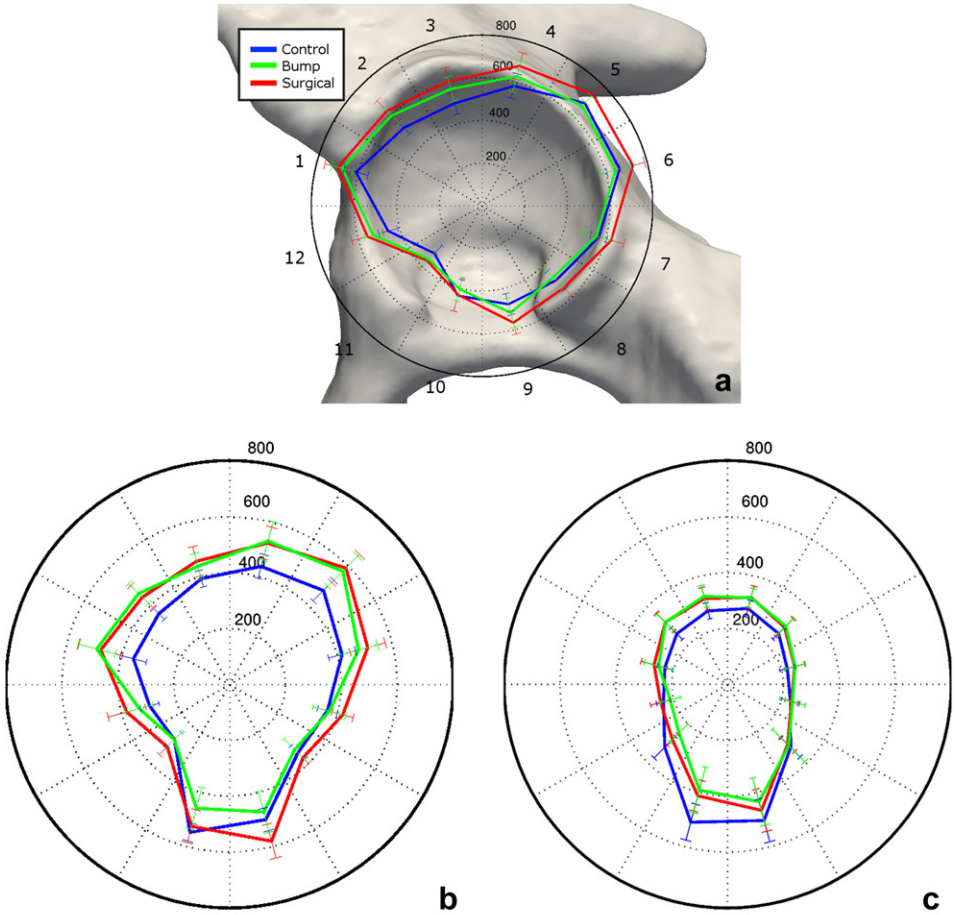

Fig. 4. BMD (mean, 95% CI) at the level of the rim (a), middle (b) and medial wall (c) in the 12 sections around the acetabulum for the three study groups. The largest differences were seen in the antero-superior region (sections 1–3) at the rim and middle levels. Section labels are shown around the circumference and values on the radial axis are mg/cc. Data shown are before adjustment for the covariate.

Table II
BMD values (mg/cc; mean ± SD) in the rim and middle levels of the antero-superior acetabulum without adjustment for the covariate

Level	Section	Group		
		Control	Bump	Surgical
Rim	1	611 ± 91	700 ± 97*	677 ± 80
	2	517 ± 61	630 ± 105*	599 ± 75*
	3	497 ± 81	604 ± 104*	566 ± 92*
Middle	1	356 ± 75	478 ± 127*	492 ± 108*
	2	358 ± 45	442 ± 91*	460 ± 79*
	3	392 ± 47	457 ± 86*	438 ± 74

* Indicates significant difference from control (ANCOVA with Sidak correction; see text for details).

mean bone density was 89–112 mg/cc higher in the Bump group (+15–22% of Control; $P = 0.001$–0.037) compared to Controls. In the Surgical group BMD in sections 2 and 3 was 69 and 81 mg/cc higher, respectively (+16% and 14% of Control; $P = 0.002$ and 0.009) compared to Controls. In section 1 of the Surgical group BMD was 66 mg/cc higher (11%) but was not significant ($P = 0.076$). Anteriorly in section 12, Bump and Surgical groups also exhibited 101 mg/cc (22%; $P = 0.009$) and 73 mg/cc (16%; $P = 0.022$) higher bone density compared to Controls, respectively.

Bone density: middle level

Differences in the middle level of the acetabulum ranged from 65 to 121 mg/cc (17–34% of Control) higher in the Bump group ($P = 0.008$–0.049) and 46–136 mg/cc (12–38%) higher in the Surgical group ($P = 0.0004$ and 0.003 in sections 1 and 2; $P = 0.091$ in section 3) over the antero-superior quadrant of the acetabulum i.e., sections 1–3 [Fig. 4(b) and Table II]. At this level the Bump group also exhibited a higher bone density in section 12 than Controls ($P = 0.005$) although the Surgical group did not ($P = 0.11$).

Bone density: medial wall level

Differences at the medial wall level ranged up to 58 mg/cc higher (18% of Control) in both the Bump and Surgical groups compared to Controls. These differences were significant in section 2 for the Bump group and sections 2 and 3 for the Surgical group [$P = 0.01$–0.043; Fig. 4(c)]. The relatively high values inferiorly are due to the thin, mainly cortical structure of this region of the pelvis.

There were no significant differences found between the Bump and Surgical groups in any region ($P > 0.073$–1.0).

When considering the acetabulum topographically, the regions of significant bone density differences are contiguous and are located in the antero-superior and adjacent regions of the acetabulum (Fig. 5). The pattern of densification was consistent in the two groups. The typical Control subject exhibited a thin layer of dense subchondral bone at the rim and over the load bearing area of the acetabulum (Fig. 6, left). In the Bump group this high-density layer appeared thicker especially near the rim, and there was an overall higher density in the deeper trabecular regions (Fig. 6, middle). The thickening of the dense subchondral layer appeared more extensive in the Surgical group subject, extending supero-medially over the weight-bearing region (Fig. 6, right). In some Surgical subjects low-density cyst-like regions were apparent in the CT but were not large enough to affect the volume-averaged density.

Bone density and alpha angle

Linear regression was performed in the rim and middle levels where bone density differences were large and cartilage damage typically occurs. Results showed significant correlations between bone density and alpha angle, measured anteriorly in the traditional 3:00 plane ($R^2 = 0.128$–0.302, $P = 0.001$–0.032; Fig. 7 and Table III). Correlations were moderately improved by including L5 in the regression model (Table III). In contrast, correlations with the 1:30 alpha angle were stronger ($R^2 = 0.104$–0.495, $P < 0.0001$–0.05; Fig. 7 and Table III) and in all cases L5 was retained in the stepwise regression, improving the correlation ($R^2 = 0.301$–0.559, $P < 0.0001$–0.004; Table III).

Bone density within subjects

In the Bump group, significant differences were found between the affected and contralateral normal side in the superior acetabulum, primarily in the middle level. In the rim level, a difference of 44 mg/cc was found in section 4 ($P = 0.046$ from Wilcoxin matched-pairs signed-ranks test; Table IV). In the middle level differences of 26–42 mg/cc were found in sections 2–5 ($P = 0.028$–0.046; Table IV). In all cases the difference was due to higher density in the affected hip.

In the Surgical group, the only difference found was in section 7 of the rim level where BMD was 39 mg/cc lower in the affected hip [95% confidence interval (CI) 1.3–77 mg/cc, $P = 0.044$].

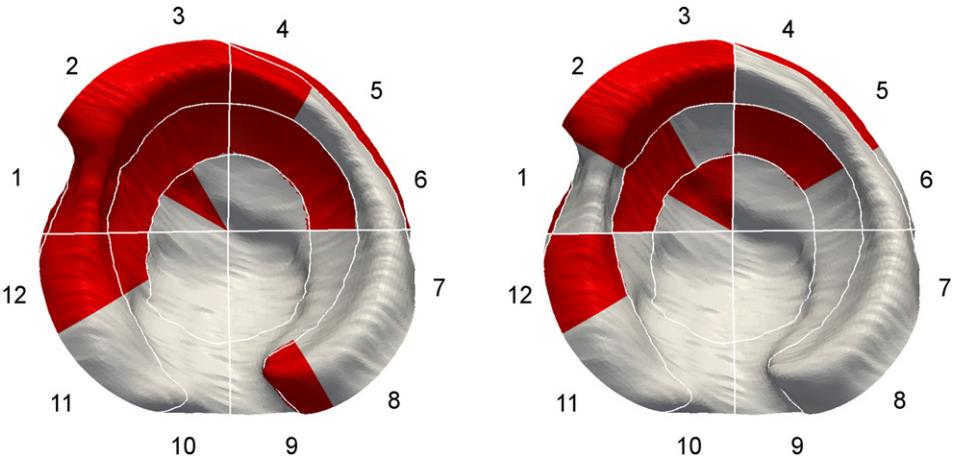

Fig. 5. BMD was significantly higher ($P < 0.05$) in regions marked red for Bump (left) and Surgical (right) compared to Controls. Wedge indices are marked. Some wedge borders are omitted for clarity.

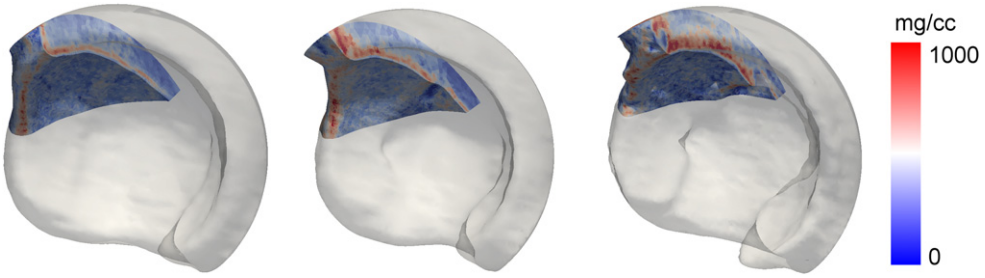

Fig. 6. Bone density distribution in the antero-superior region in a typical Control (left), Bump (middle) and Surgical (right) subject. The Bump subject exhibited a thicker high-density region of subchondral bone, especially near the rim. The Surgical subject exhibited an increased thickness and more extensive region of high-density subchondral bone.

Discussion

This study compared the subchondral BMD in subjects with symptomatic or asymptomatic cam deformities compared to controls and examined the relationship between BMD and the alpha angle. Both groups with cam deformities, i.e., Bump and Surgical, were found to have elevated bone density compared to the Control group. Early bone changes have been associated with knee arthritis[8]. The similarity between the asymptomatic Bump and symptomatic Surgical groups, both with higher bone density compared to Controls, suggests that joint degeneration may have already begun in subjects in the Bump group although below the threshold for causing clinical symptoms. Interestingly, a previous study using single-photon emission CT (SPECT) showed focal uptake in the bone of both symptomatic and asymptomatic FAI subjects[19], suggesting active remodelling of the subchondral bone in these patients. Subjects in the current study groups had a morphological cam deformity at the anterior or antero-superior femoral head–neck junction as measured by the alpha angle[11]. As such, pathologic contact between the cam deformity and the acetabular rim, labrum, chondrolabral junction and cartilage is expected to occur in the antero-superior acetabulum during certain hip motions, corresponding to the location of cartilage damage and delamination seen intraoperatively[10]. In the current study the largest differences in bone density were seen in the antero-superior quadrant, i.e., wedges 1–3, for both deformity groups compared to normal controls as expected (Figs. 4 and 5). Interestingly the region of elevated bone density also extended somewhat antero-inferiorly as well as posteriorly for both groups (Fig. 5). Furthermore, within-subject comparisons of Bump subjects showed higher BMD in the hip with a cam deformity compared with the contralateral normal hip. Within-subject comparisons of Surgical subjects showed that BMD was generally similar in symptomatic and asymptomatic bilateral cam deformities. These results support the hypothesis that elevated BMD is associated with cam-type FAI deformities.

This study examined BMD in 36 regions around the acetabulum. Results are presented for individual application of ANCOVA tests within each region with no correction for these 36 tests, although *post-hoc* corrections were made within each region for multiple comparisons between groups. Inclusion of section and level in a more complex multi-factor model may provide more rigorous statistical tests. However density is expected to vary continuously throughout the pelvis such that correlation of BMD between regions is high for regions that are close together. Lack of a statistical test that can account for spatial relationships between regions is a limitation of this study. Although from a purely statistical perspective this may lead to spurious results, the regions of significant differences are concentrated in the antero-superior region and are mostly contiguous. This supports the a priori hypothesis that bone density is higher in this region due to the associated impingement and decreases the chance of Type I errors.

Although subjects are expected to exhibit general bone density differences, which may be due to many factors such as age, body weight, diet and activity level, bone density within the spine was included as a covariate to minimize this influence. After adjusting for the covariate, differences between Bump and Surgical groups compared to Controls better reflect potential consequences of the cam deformity on the antero-superior acetabulum. The elevated bone density may be a result of elevated stresses in the rim due to impingement, which triggers a bone remodelling response[20]. Elevated stresses could be explained as a stress concentration due to the shape of the deformity or similar stiffening of the subchondral bone on the femoral side. Alternatively, bone changes could be a reaction to pro-inflammatory cytokines[21] that may be released from labrum cells[22] as the labrum is deformed by impingement. One explanation for increased bone density outside the presumed region of impingement may be that permeation of biochemical signals from an active remodelling bone region induces a somewhat decentralized response.

This study found significant correlations between bone density in the antero-superior acetabulum and the alpha angle measured at the

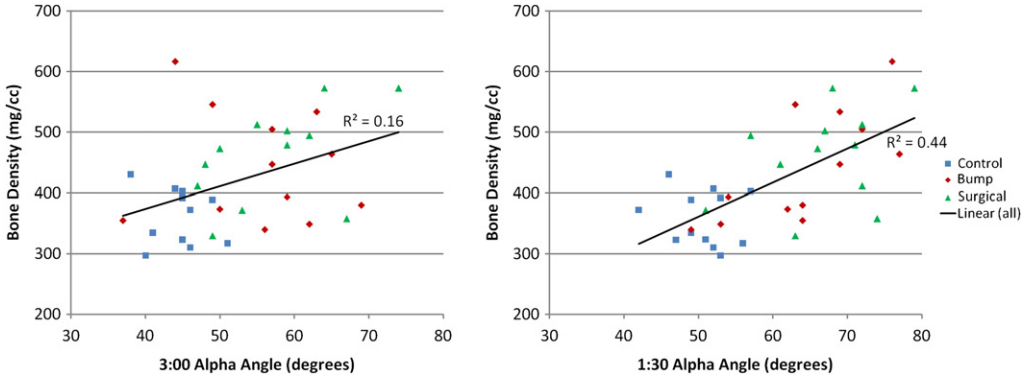

Fig. 7. Correlation of BMD and the alpha angle measured in the 3:00 plane (left) was lower than for the alpha angle measured in the 1:30 plane (right). Data shown are before adjusting for the covariate which improved the correlation (see text).

Table III
Coefficient of determination (R^2) from step-wise linear regression of BMD vs alpha angle and L5 in the rim and middle levels of the antero-superior acetabulum

Level	Section	3:00 Alpha		1:30 Alpha	
		Alpha	Alpha + L5	Alpha	Alpha + L5
Rim	12	0.277	0.390	0.200	0.345
	1	0.251	0.251*	0.212	0.301
	2	0.128	0.288	0.257	0.472
	3	N/S	0.285	0.148	0.404
	4	0.132	0.369	0.104	0.377
Middle	12	0.222	0.302	0.164	0.313
	1	0.302	0.302*	0.495	0.554
	2	0.159	0.159*	0.437	0.559
	3	N/S	N/S	0.238	0.367
	4	0.212	0.326	0.309	0.471

All correlations were significant ($P < 0.05$) except as noted (N/S, where $P = 0.10$–0.14).
R^2 is also shown from simple linear regression of BMD vs alpha for comparison.
* Indicates L5 was not retained in the step-wise model due to a non-significant change in the F-statistic.

anterior and antero-superior femoral head–neck junction ($P < 0.05$; Fig. 7). The 3:00 alpha angle is the traditional measure of the cam deformity and is used clinically as a risk factor for impingement[16]. It is known that the cam deformity is largest, with higher alpha angle, in the antero-superior location as opposed to anterior location[14,23]. It is expected that this location is more likely to interact with the acetabular labrum and rim which may explain the stronger correlation between bone density and the alpha angle measured in the 1:30 plane (largest $R^2 = 0.559$ with L5 included) compared to the traditional 3:00 plane (largest $R^2 = 0.302$). Furthermore, measurement in the 1:30 plane is more likely to assess the deformity near the epicentre, whereas the 3:00 plane assesses the deformity nearer the periphery[14], and therefore better quantifies the severity of the deformity. Thus the antero-superior alpha angle may prove to be more clinically useful in predicting early joint degeneration in cam-type FAI than the traditional 3:00 or anterior alpha angle, as originally proposed by Nötzli *et al.*[11] The prognosis of asymptomatic deformities is currently difficult to predict, however some may eventually develop symptoms[19]. A threshold alpha angle of 50° in the 3:00 plane is frequently used to classify a head–neck contour as abnormal[11,16,24] since it agrees well with intraoperative findings[16]. However a complete three-dimensional analysis that considers shape of the deformity, the acetabulum as well as hip motions is required to better understand the relationship between deformity characteristics and degeneration.

The resolution provided by the clinical CT scanner used in the study allowed only macroscopic analysis of bone density and precluded assessment of subchondral architecture. Furthermore, subchondral compact bone could not be assessed independent of adjacent trabecular bone due to the image resolution. Previous reports have suggested that subchondral bone actively remodels in arthritic joints[1,19,25]. Increased stiffness of subchondral cancellous bone induced cartilage loss in canines[26] and was associated with osteoarthritis in the medial tibial compartment in humans[27]. The pattern of bone density changes may be complex and depend on the pathomechanism. In actively remodelling bone, which may occur in FAI subjects[19] and has been observed in osteoarthritis[1,25], the delay in mineralization of the osteoid results in a lower tissue modulus[25]. However, an increase in the number or thickness of trabeculae could make up for the lower tissue modulus, resulting in a comparable bone apparent modulus[25]. In this study an overall increase in bone density was found as assessed by qCT to a depth that included compact and cancellous bone. Bone density measured from qCT is highly correlated with the elastic modulus, having a coefficient of determination (R^2) of 0.924[28]. The resulting power–law relationship has an exponent of 2.25[28]. Thus the 20–40% increase in CT density is expected to result in an approximately 50–110% increase in the apparent modulus of the subchondral bone. In a simplified elastic model, doubling of the subchondral bone plate stiffness was found to increase the surface tensile stresses in cartilage by 57% but deep shear stress by only 2.6%[29]. More complex material models of cartilage such as fibril-reinforced poroelastic models[30,31] may provide more information on stresses within the structural components of cartilage tissue that may influence cellular activity or cause direct tissue damage. Furthermore, the influence of the increased subchondral bone stiffness on the clinical performance of surgical repair techniques of cartilage needs careful consideration.

Although it has been shown that bone turnover can precede cartilage biochemical changes in a cartilage injury model[9], the sequence of bone and cartilage changes associated with cam-type FAI is not known. Recently-developed quantitative magnetic resonance imaging (MRI) techniques have shown differences in glycosaminoglycan content of acetabular cartilage in FAI subjects and were correlated with the alpha angle[32]. Similar assessment of the subjects in this study, using $T_{1\rho}$ MRI, is on-going[33] and comparison of subchondral bone and cartilage results will provide further insight into the sequence of degenerative changes associated with cam FAI. Furthermore, examination of subchondral bone density on the femoral side will improve understanding of the contact mechanics involved in FAI.

Table IV
Mean BMD differences between the affected and normal contralateral hip in a subgroup of Bump subjects in the superior acetabulum ($n = 6$)

Level	Section	Mean difference (mg/cc)	*P*-value
Rim	1	10.2	0.46
	2	28.4	0.17
	3	17.9	0.46
	4	44.3	**0.046**
	5	34.4	0.075
	6	6.3	0.46
Middle	1	18.4	0.25
	2	41.8	**0.028**
	3	26.4	**0.046**
	4	39.8	**0.028**
	5	31.1	**0.028**
	6	6.9	0.60

P values from Wilcoxin matched-pairs signed-rank tests are shown in the last column with significant values in bold. All differences are positive indicating BMD in the affected side was higher than the contralateral side.

Conclusions

Bone density was elevated in cam-FAI subjects compared to control subjects, regardless of symptom status, and these differences were primarily confined to the rim and middle levels. Antero-superior subchondral BMD in the acetabulum had higher correlation with the alpha angle measured in the 1:30 plane than in the traditional 3:00 plane and therefore may provide a more useful assessment for the understanding of pathomechanisms of impingement than traditional alpha angle. Follow-up assessment of the asymptomatic deformities and further work to understand the interaction of the cam deformity with the acetabulum is required to determine the deformity characteristics that lead to joint degeneration.

Contributions

All authors contributed to the conception and design of the study. AS and HF contributed to data analysis. PB, KR and MS provided technical and clinical data interpretation. PB provided study patients. An initial draft was provide by AS and critically reviewed by all other authors.

Funding sources
The study was supported by an unrestricted grant from the Canadian Institutes of Health Research.

Conflicts of interest
The authors have no conflicts of interest related to this study.

Acknowledgements

The authors thank Tim Ramsay for his help with the statistical methods.

References

1. Brandt KD, Dieppe P, Radin EL. Etiopathogenesis of osteoarthritis. Rheum Dis Clin North Am 2008;34:531–59.
2. Fernandez-Madrid F, Karvonen RL, Teitge RA, Miller PR, An T, Negendank WG. Synovial thickening detected by MR imaging in osteoarthritis of the knee confirmed by biopsy as synovitis. Magn Reson Imaging 1995;13:177–83.
3. Radin EL, Martin RB, Burr DB, Caterson B, Boyd RD, Goodwin C. Effects of mechanical loading on the tissues of the rabbit knee. J Orthop Res 1984;2:221–34.
4. Kellgren JH, Lawrence JS. Radiological assessment of osteoarthritis. Ann Rheum Dis 1957;16:494–502.
5. Tönnis D. Normal values of the hip joint for the evaluation of X-rays in children and adults. Clin Orthop Relat Res 1976;119:39–47.
6. Nelson AE, Braga L, Renner JB, Atashili J, Woodard J, Hochberg MC, *et al*. Characterization of individual radiographic features of hip osteoarthritis in African American and White women and men: the Johnston County Osteoarthritis Project. Arthritis Care Res 2010;62:190–7.
7. Nevitt MC, Lane NE, Scott JC, Hochberg MC, Pressman AR, Genant HK, *et al*. Radiographic osteoarthritis of the hip and bone mineral density. The Study of Osteoporotic Fractures Research Group. Arthritis Rheum 1995;38:907–16.
8. Shamir L, Ling SM, Scott W, Hochberg M, Ferrucci L, Goldberg IG. Early detection of radiographic knee osteoarthritis using computer-aided analysis. Osteoarthritis Cartilage 2009;17:1307–12.
9. Newberry WN, Zukosky DK, Haut RC. Subfracture insult to a knee joint causes alterations in the bone and in the functional stiffness of overlying cartilage. J Orthop Res 1997;15:450–5.
10. Ganz R, Leunig M, Leunig-Ganz K, Harris WH. The etiology of osteoarthritis of the hip: an integrated mechanical concept. Clin Orthop Relat Res 2008;466:264–72.
11. Nötzli HP, Wyss TF, Stoecklin CH, Schmid MR, Treiber K, Hodler J. The contour of the femoral head-neck junction as a predictor for the risk of anterior impingement. J Bone Joint Surg Br 2002;84:556–60.
12. Hack K, Di Primio G, Rakhra K, Beaulé PE. Prevalence of cam-type femoroacetabular impingement morphology in asymptomatic volunteers. J Bone Joint Surg Am 2010;92:2436–44.
13. Allen D, Beaulé PE, Ramadan O, Doucette S. Prevalence of associated deformities and hip pain in patients with cam-type femoroacetabular impingement. J Bone Joint Surg Br 2009;91:589–94.
14. Rakhra KS, Sheikh AM, Allen D, Beaule PE. Comparison of MRI alpha angle measurement planes in femoroacetabular impingement. Clin Orthop Relat Res 2009;467:660–5.
15. Tannast M, Siebenrock KA, Anderson SE. Femoroacetabular impingement: radiographic diagnosis – what the radiologist should know. AJR Am J Roentgenol 2007;188:1540–52.
16. Barton C, Salineros MJ, Rakhra KS, Beaulé PE. Validity of the alpha angle measurement on plain radiographs in the evaluation of cam-type femoroacetabular impingement. Clin Orthop Relat Res 2011;469:464–9.
17. Sutter R, Dietrich TJ, Zingg PO, Pfirrmann CWA. How useful is the alpha angle for discriminating between symptomatic patients with cam-type femoroacetabular impingement and asymptomatic volunteers? Radiology 2012;264:514–21.
18. Lubovsky O, Peleg E, Joskowicz L, Liebergall M, Khoury A. Acetabular orientation variability and symmetry based on CT scans of adults. Int J Comput Assist Radiol Surg 2010;5:449–54.
19. Matar WY, May O, Raymond F, Beaulé PE. Bone scintigraphy in femoroacetabular impingement: a preliminary report. Clin Orthop Relat Res 2009;467:676–81.
20. Wolff J. Das Gesetz der Transformation der Knochen. Berlin: Verlag von August Hirschwald; 1892.
21. Zupan J, Komadina R, Marc J. The relationship between osteoclastogenic and anti-osteoclastogenic pro-inflammatory cytokines differs in human osteoporotic and osteoarthritic bone tissues. J Biomed Sci 2012;19:28.
22. Dhollander AAM, Lambrecht S, Verdonk PCM, Audenaert EA, Almqvist KF, Pattyn C, *et al*. First insights into human acetabular labrum cell metabolism. Osteoarthritis Cartilage 2012;20:670–7.
23. Pfirrmann CWA, Mengiardi B, Dora C, Kalberer F, Zanetti M, Hodler J. Cam and pincer femoroacetabular impingement: characteristic MR arthrographic findings in 50 patients. Radiology 2006;240:778–85.
24. Nepple JJ, Martel JM, Kim Y-J, Zaltz I. Clohisy JC. Do plain radiographs correlate with CT for imaging of cam-type femoroacetabular impingement? Clin Orthop Relat Res 2012;470:3313–20.
25. Day JS, Ding M, van der Linden JC, Hvid I, Sumner DR, Weinans H. A decreased subchondral trabecular bone tissue elastic modulus is associated with pre-arthritic cartilage damage. J Orthop Res 2001;19:914–8.
26. Ewald FC, Poss R, Pugh J, Schiller AL, Sledge CB. Hip cartilage supported by methacrylate in canine arthroplasty. Clin Orthop Relat Res 1982:273–9.
27. Madsen OR, Schaadt O, Bliddal H, Egsmose C, Sylvest J. Bone mineral distribution of the proximal tibia in gonarthrosis assessed in vivo by photon absorption. Osteoarthritis Cartilage 1994;2:141–7.
28. Les CM, Keyak JH, Stover SM, Taylor KT, Kaneps AJ. Estimation of material properties in the equine metacarpus with use of quantitative computed tomography. J Orthop Res 1994;12:822–33.
29. Wei H-W, Sun S-S, Jao S-HE, Yeh C-R, Cheng C-K. The influence of mechanical properties of subchondral plate, femoral head and neck on dynamic stress distribution of the articular cartilage. Med Eng Phys 2005;27:295–304.
30. Chegini S, Ferguson SJ. Time and depth dependent Poisson's ratio of cartilage explained by an inhomogeneous orthotropic fiber embedded biphasic model. J Biomech 2010;43:1660–6.
31. Li LP, Cheung JTM, Herzog W. Three-dimensional fibril-reinforced finite element model of articular cartilage. Med Biol Eng Comput 2009;47:607–15.
32. Pollard TCB, McNally EG, Wilson DC, Wilson DR, Mädler B, Watson M, *et al*. Localized cartilage assessment with three-dimensional dGEMRIC in asymptomatic hips with normal morphology and cam deformity. J Bone Joint Surg Am 2010;92:2557–69.
33. Rakhra KS, Lattanzio P-J, Cárdenas-Blanco A, Cameran IG, Beaulé PE. Can T1-rho MRI detect acetabular cartilage degeneration in femoroacetabular impingement? J Bone Joint Surg Br, 2012;94:1187–92.